Cellular/Molecular

Origin of Inner Ear Hair Cells: Morphological and Functional Differentiation from Ciliary Cells into Hair Cells in Zebrafish Inner Ear

Masashi Tanimoto, Yukiko Ota, Maya Inoue, and Yoichi Oda
Division of Biological Science, Graduate School of Science, Nagoya University, Nagoya 464-8602, Japan

Auditory and vestibular functions in vertebrates depend on the transduction of sound vibration or head acceleration into electrical responses in inner ear hair cells. Mechanoelectrical transduction occurs at the tip of stereocilia, which are polarized to form an orientational arrangement that determines directional sensitivity. It remains to be clarified when and how premature hair cells acquire their specialized structure and function in living animals. The developmental origin of inner ear hair cells has been studied *in vivo* in zebrafish embryos. Tether cells, a small number of ciliated cells associated with an "ear stone" (or otolith) in the embryonic zebrafish inner ear, are believed to be precocious hair cells. However, whether or not tether cells acquire hair bundles and mechanosensitivity remains unknown. In the present study, we investigated the morphological and functional development of tether cells. Immunohistochemical examination revealed that stereocilia appeared on the tether cell apex in a polarized arrangement at 22 h postfertilization (hpf). Labeling with FM1-43, a marker of functional mechanotransduction channels, and the *in vivo* electrophysiological recording of mechanotransducer responses in the developing inner ear demonstrated that tether cells acquired direction-selective mechanosensitivity at 23 hpf. These results revealed that tether cells begin to function as hair cells within an hour after the appearance of a polarized array of stereociliary bundles. Thus, the ciliary cells morphologically and functionally differentiate into the first sensory hair cells in the inner ear of the zebrafish.

Introduction

Detection of sound and head acceleration in vertebrates depends on the transduction of mechanical force into electrical signals in inner ear hair cells (Hudspeth, 1989). Hair bundles on the apical surface of hair cells are specialized structures that are necessary to detect mechanical force. Each hair bundle comprises a bundle of actin-based stereocilium associated with a single microtubule-based kinocilium, although kinocilia disappear postnatally in murine and chicken cochlea (Zine and Romand, 1996). The stereocilia are arranged by height to form a staircase-like pattern, and the kinocilium is located next to the tallest edge of the stereocilia. The orientational arrangement of the hair bundles determines the functional polarity of the hair cells (Shotwell et al., 1981): deflection of the hair bundle toward longer stereocilia (positive deflection) opens mechanotransduction channels at their tips (Beurg et al., 2009), leading to depolarization of the hair cells (Hudspeth and Jacobs, 1979).

Developmental acquisition of hair bundles and mechanotransduction in inner ear hair cells has been studied *in vitro* in higher vertebrates, and the origin of hair cells has been discussed extensively (see Discussion). *In vivo* observation of embryonic inner ear in zebrafish has morphologically shown that a small number of specialized ciliary cells in otic vesicles are premature hair cells (Riley et al., 1997) (see below). It remains unknown, however, whether or not (and when) a directional array of hair bundles and mechanotransduction appear in the ciliary cells.

As in other vertebrates, the macula appears as the first sensory patch in the zebrafish otic vesicle (Whitfield et al., 2002). The macula contains receptor hair cells coupled to a calcium carbonate crystal, known as an otolith, and detects linear acceleration and sound vibration (Popper and Fay, 1993; Nicolson, 2005). Hair cells with stereocilia are morphologically identified in anterior (utricular) and posterior (saccular) maculae at 1 d postfertilization (Haddon and Lewis, 1996; Haddon et al., 1999). Uptake of FM1-43, a fluorescent dye that enters hair cells through mechanotransduction channels (Meyers et al., 2003), indicated that mechanosensitive channels are already localized on the hair cells by 27 hpf (Tanimoto et al., 2009). Furthermore, mechanical displacement of the otolith evoked microphonic potentials, which reflect current flow into hair cells through the mechanotransduction channels (Hudspeth, 1982), in the otic vesicle at 27 hpf (Tanimoto et al., 2009).

It should be noted that before this period, critical developmental events occur in the otic vesicle (Riley et al., 1997; Colantonio et al., 2009). Over 100 ciliated cells appear in the epithelium around 19 hpf. The ciliary cells are morphologically classified into two groups. In most of the cells, ciliary length gradually decreases to 1–2 μm by 24 hpf, and the cells subsequently lose

Received Oct. 22, 2010; revised Dec. 21, 2010; accepted Jan. 21, 2011.

This work was supported by Grants-in-Aid for Scientific Research (19650099 and 22300126 to Y.O.), Global Centers of Excellence Program "Advanced Systems-Biology: Designing The Biological Function" from the Ministry of Education, Culture, Sports, Science and Technology, and a Japan Society for the Promotion of Science Fellowship to M.T.

Correspondence should be addressed to either Masashi Tanimoto or Yoichi Oda, Division of Biological Science, Graduate School of Science, Nagoya University, Furo-cho, Chikusa, Nagoya 464-8602, Japan. E-mail: m-tanimoto@bio.nagoya-u.ac.jp or oda@bio.nagoya-u.ac.jp.

DOI:10.1523/JNEUROSCI.5554-10.2011

 0270-6474/11/313784-11$15.00/0

their cilia. In contrast, a few ciliated cells, located at the anterior and posterior ends of the otic vesicle, anchor the otolith to their tips by 21.5 hpf, and increase in ciliary length: these cells are referred to as tether cells. Based on cell number, shape, location, and tubulin immunoreactivity in the cell body, tether cells have been shown to be precociously forming hair cells (Riley et al., 1997). However, neither the appearance of stereociliary bundles and their orientation nor the electrophysiological properties of tether cells have been clarified thus far.

Here, we investigated the morphological and functional development of tether cells in zebrafish embryos by immunohistochemical staining of kinocilia and stereocilia, by labeling hair cells with FM1-43, and by *in vivo* electrophysiological recording of mechanotransduction responses.

Materials and Methods

Animals. Wild-type zebrafish, *Danio rerio*, were maintained under standard conditions. Embryos of either sex were reared in fresh fish water at 28.5°C and were staged according to hpf. The developmental stage of each embryo before the 30-somite stage (24 hpf) was determined according to somite formation (Hanneman and Westerfield, 1989; Kimmel et al., 1995) immediately before every experiment. Embryos were dechorionated manually using fine forceps. All procedures complied with guidelines stipulated by the Nagoya University Committee on Animal Research.

Immunohistochemical labeling of hair bundles. Embryos were fixed in 4% paraformaldehyde in 0.1 M PBS at 4°C overnight. Samples were permeabilized with acetone for 10 min at −20°C and then incubated in blocking solution containing 1% BSA and 0.1% DMSO in 0.1 M PBS for 1 h at room temperature. To visualize the kinocilia of hair cells, a 1:100 dilution of antibody directed against acetylated-tubulin (T6793; Sigma-Aldrich) was used as the primary antibody with a 4°C, overnight incubation. The primary antibody was detected with a 1:2000 dilution of Alexa 488-conjugated goat anti-mouse IgG (A11001; Invitrogen) at room temperature for 3 h, or at 4°C overnight. Simultaneously, hair cell stereocilia were visualized with a 1:200 dilution of Alexa 568-conjugated phalloidin (A12380; Invitrogen).

FM1-43 labeling of hair cells. To label hair cells with a styryl dye, 40 μM FM1-43FX (fixable analog of FM1-43 (*N*-(3-triethylammoniumpropyl)-4-(4-(dibutylamino)styryl) pyridinium dibromide), Invitrogen) dissolved in extracellular solution (see below) was injected into the lumen of the otic vesicle through a micropipette (Corey et al., 2004; Tanimoto et al., 2009).

Confocal imaging of labeled embryos. Whole embryos, immunostained or labeled with FM1-43FX, were mounted in 1.2% low-melting-point agar, or held on a Sylgard-coated dish with tungsten pins. Three-dimensional morphological data were obtained using a confocal laser-scanning microscope (FV300; Olympus) at 0.3–0.5 μm *z*-axis intervals with a 60× water-immersion objective (numerical aperture: 0.90, Olympus) and with data-acquisition software (Fluoview; Olympus). For observation of immunostained specimens, data were collected using a sequential-scan mode to obtain green and red signals separately.

To measure the ciliary lengths, whole animals stained immunohistochemically were tilted so that hair bundles were imaged from the side. The length of a cilium was measured from base to tip in a *z*-series stack with three-dimensional reconstruction. Because of the difficulty in determining the base of the stereocilia, the length of the stereocilia was measured from the base of the kinocilium to the stereociliary tip. For 20–24 hpf embryos, cilia located within 15 μm of anterior tether cells were analyzed.

To define the orientation of hair bundles, whole embryos were viewed from the apical side of each sensory epithelium. The orientation was determined by drawing a line through the center of the stereociliary base and the base of the kinocilium. Orientation angles were measured from the midline of the head. Data were expressed as mean ± SD unless otherwise noted.

In vivo *electrophysiological recordings.* Electrophysiological recordings were performed as described previously (Tanimoto et al., 2009) with some modification. Experiments were performed at 25–28°C. Embryos were temporarily anesthetized in 0.2% tricaine methanesulfonate (MS-222) (Sigma-Aldrich), pinned on a Sylgard-coated glass-bottomed dish, and then covered with extracellular solution containing (in mM) 134 NaCl, 2.9 KCl, 1.2 $MgCl_2$, 2.1 $CaCl_2$, 10 HEPES, and 10 glucose, adjusted to pH 7.8 with NaOH. The concentration of MS-222 was kept below 0.002% during recordings. The preparations were observed using a 40× or 60× water-immersion objective on a microscope (BX51WI; Olympus).

Recording microelectrodes were pulled from borosilicate glass (GD-1.5; Narishige) and filled with extracellular solution (pipette resistance, 5–10 MΩ). The microelectrode was inserted into the otic vesicle, and the electrode tip was placed within ~10 μm from the otolith center, except where otherwise noted. A stiff glass probe (1 μm tip diameter) attached to a piezoelectric stack actuator (AE0505D08F; NEC TOKIN Corporation) was used to produce a mechanical displacement of otoliths associated with the tips of tether cell cilia. Because the otolith at this early developmental stage is not very sticky, it does not adhere to the glass probe. Therefore, to move the otolith toward the lateral or medial side in the otic vesicle, the glass probe was moved transversely, vertically to the probe axis. Voltage waveforms for driving the actuator were generated by an arbitrary function generator (DF1906; NF Corporation) with software (DF0106; NF Corporation) and amplified with a piezo-driver amplifier (HJPZ-0.15P; Matsusada Precision Inc.). The rise time of the waveform was set at 5 ms to keep the stimulus probe in contact with the otolith, which tends to separate when moved rapidly. The voltage-displacement relationship of the piezoelectric actuator was measured using a laser displacement meter (LK-G5000; Keyence) (supplemental Fig. S1, available at www.jneurosci.org as supplemental material). To calibrate the motion of the probe tip and the otolith, video images were recorded using a high-speed camera (Fastcam Ultima 1024; Photron) at 4000 frames per second. Microphonic potentials were recorded at 20 kHz using a MultiClamp 700B amplifier (Molecular Devices), and analyzed with Clampfit 10.2 software (Molecular Devices). To record the responses of the anterior macular hair cells, the posterior otolith was removed from the posterior macula using a stimulus glass probe to avoid possible contamination with responses of the posterior macular hair cells. Conversely, the anterior otolith was removed from the anterior macula to record the responses of the posterior macular hair cells (see Results). To block mechanotransduction channels pharmacologically (Gale et al., 2001), 40 μM FM1-43FX diluted in the extracellular solution was injected into the otic vesicle.

Results

Macular hair cells possess a polarized arrangement of hair bundles at 27 hpf

A previous study showed that cilia and somata of macular hair cells at 27 hpf were labeled with FM1-43, and that microphonic potentials were observed in the otic vesicle in response to the mechanical displacement of otoliths associated with hair bundles (Tanimoto et al., 2009). This suggests that hair cells are morphologically developed and functional at this stage.

In the present study, we demonstrated the presence of kinocilia and stereocilia in macular hair cells at 27 hpf by immunohistochemical staining with an anti-acetylated tubulin antibody and fluorescent phalloidin. Macular hair cells are located at the anteroventral and posteroventral parts of the otic vesicle. The anti-acetylated tubulin antibody labeled a small number of kinocilia projecting into the lumen of the otic vesicle (Fig. 1). The apical cytoplasm of the hair cells was also stained with the antibody (Fig. 1, asterisks, 33 of 35 cells), and each kinocilium was associated with a bundle of stereocilia labeled with fluorescent phalloidin. Thus, hair cells with a kinocilium and stereocilia were identified at 27 hpf. The number of hair cells at 27 hpf was 2.7 ± 1.1 in the anterior macula and 2.1 ± 0.4 in the posterior macula (5 fish, summarized data from bilateral otic vesicles). The length of the

kinocilium and stereocilia was 6.7 ± 0.8 μm and 2.8 ± 0.7 μm, respectively (23 cells).

A polarized arrangement of hair bundles in each hair cell determines the directional sensitivity to acceleration or vibratory stimulus. Next, we examined the direction of hair-bundle polarity by observing each macula dorsally to view the apical side of hair cells. Posterior macular hair cells were also observed laterally since they are located on a curved sensory epithelium in the ventromedial part of the otic vesicle at 27 hpf; the posterior macula gradually relocates to the medial wall of the otic vesicle from the ventral part as the otic capsule develops (Haddon et al., 1999; Whitfield et al., 2002). The phalloidin-labeled stereocilia on the apex of the hair cells exhibited eccentric, dark, unlabeled spots where the kinocilium was located (Fig. 2*B–D*). Hair-bundle polarity was determined by the arrangement of kinocilium and stereocilia (Fig. 2*D*, inset). At 27 hpf, the polarity of the anterior macular hair cells was oriented laterally (Fig. 2*E*, *G*; left: 263 ± 22°, 17 cells; right: 91 ± 33°, 13 cells), as observed previously in 30 hpf embryos (Haddon et al., 1999). In the posterior macula, hair-bundle polarity was pointing in the posterolateral direction (Fig. 2*G*, left: 236 ± 20°, 17 cells; right: 138 ± 22°, 12 cells); when viewed laterally, they were oriented in the posteroventral direction (Fig. 2*F*, *G*; left: 192 ± 8°, 7 cells; right: 207 ± 12°, 10 cells). These data reveal that the hair bundles are unidirectionally oriented in each macula at 27 hpf.

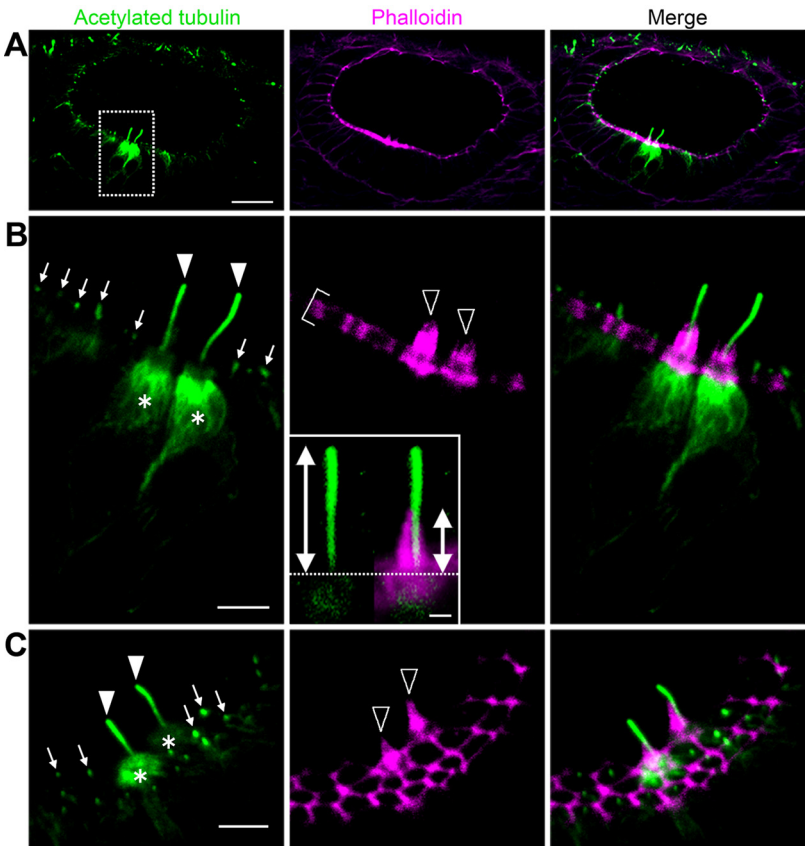

Figure 1. Macular hair cells possess kinocilia and stereocilia at 27 hpf. ***A***, Lateral view of the otic vesicle in an embryo double-stained with an anti-acetylated tubulin antibody (green) and fluorescent phalloidin (magenta) at 27 hpf. Anterior macular hair cells are located at the anteroventral part of the lumen. Dotted square in ***A*** is highlighted in ***B***. ***B***, ***C***, Ciliary bundles were observed at the anterior (***B***) and posterior (***C***) macular hair cells. A single, long kinocilium in each hair cell was stained with an anti-acetylated tubulin antibody (filled arrowheads), and a bundle of stereocilia was labeled with fluorescent phalloidin (open arrowheads). Anti-acetylated tubulin antibody also labeled the apical part of the cell bodies of hair cells (asterisks) and short cilia on cells around the hair cells (arrows). Fluorescent phalloidin stained cortical actin (bracket). Inset in ***B***, Length of the kinocilium (green) and stereocilia (magenta), indicated by arrows, was measured from the base of the kinocilium. Anterior is to the left and dorsal is up in all of the figures. Scale bars: ***A***, 20 μm; ***B***, ***C***, 5 μm; inset in ***B***, 1 μm.

Macular hair cells respond selectively to a positive deflection of hair bundles at 27 hpf

We also examined the mechanosensitivity of hair cells at 27 hpf through the *in vivo* recording of microphonic potentials in response to the displacement of the otolith with a stiff glass probe driven by a piezoelectric actuator. Microphonic potentials, which are field potentials obtained in the inner ear, reflect current flow through the mechanotransduction channels located at the hair-bundle tips (Hudspeth, 1982). As exemplified in Figure 3*A*, deflection of the anterior otolith toward the lateral side (positive displacement) evoked a remarkable and transient negative potential, followed by a sustained negative potential in the otic vesicle, suggesting that an adaptation mechanism immediately attenuates the mechanotransduction response. The decay time course of the mechanically evoked potential was fit by a single-order, exponential function, with a time constant of 5.4 ± 1.2 ms (Fig. 3*A*, 8 fish, step size ~0.5 μm). In contrast, deflection of the otolith in the medial direction (negative displacement) did not evoke significant potentials (Fig. 3*B*). The evoked responses were blocked after FM1-43, a permeant blocker of mechanotransduction channels (Gale et al., 2001), was injected into the otic vesicle and incorporated by the hair cells (Fig. 3*C*). Plots of the amplitude versus otolith displacement were well fit by a Boltzmann function (Fig. 3*D*). The operating range of displacement corresponding to 10–90% of the maximal response was 1.1 ± 0.3 μm (8 fish), and the resting open probability of mechanotransduction channels was estimated to be 6.4 ± 3.8% (8 fish). Because microphonic potentials are extracellular field potentials, their size and shape might depend on the recording sites (Hudspeth, 1982). However, potentials obtained from various locations in the otic vesicle were similar in amplitude as well as waveform, indicating that the mechanotransduction currents produce ubiquitous field potentials inside the embryonic otic vesicle (Fig. 3*E–G*, 3 fish). Corresponding to morphological observations, these data demonstrate that macular hair cells at 27 hpf possess functionally polarized hair bundles that respond selectively to positive deflection.

Tether cells develop into the first macular hair cells in the inner ear

Next, we investigated the developmental origin of macular hair cells. A previous study suggested that a special type of ciliated cells, referred to as tether cells, are premature macular hair cells in zebrafish; the tether cells are located at the anterior and posterior ends of the otic vesicle (Riley et al., 1997). It has been shown that cilia and apical cell bodies of the tether cells are immunopositive for anti-acetylated tubulin, whereas somata of other ciliated cells are

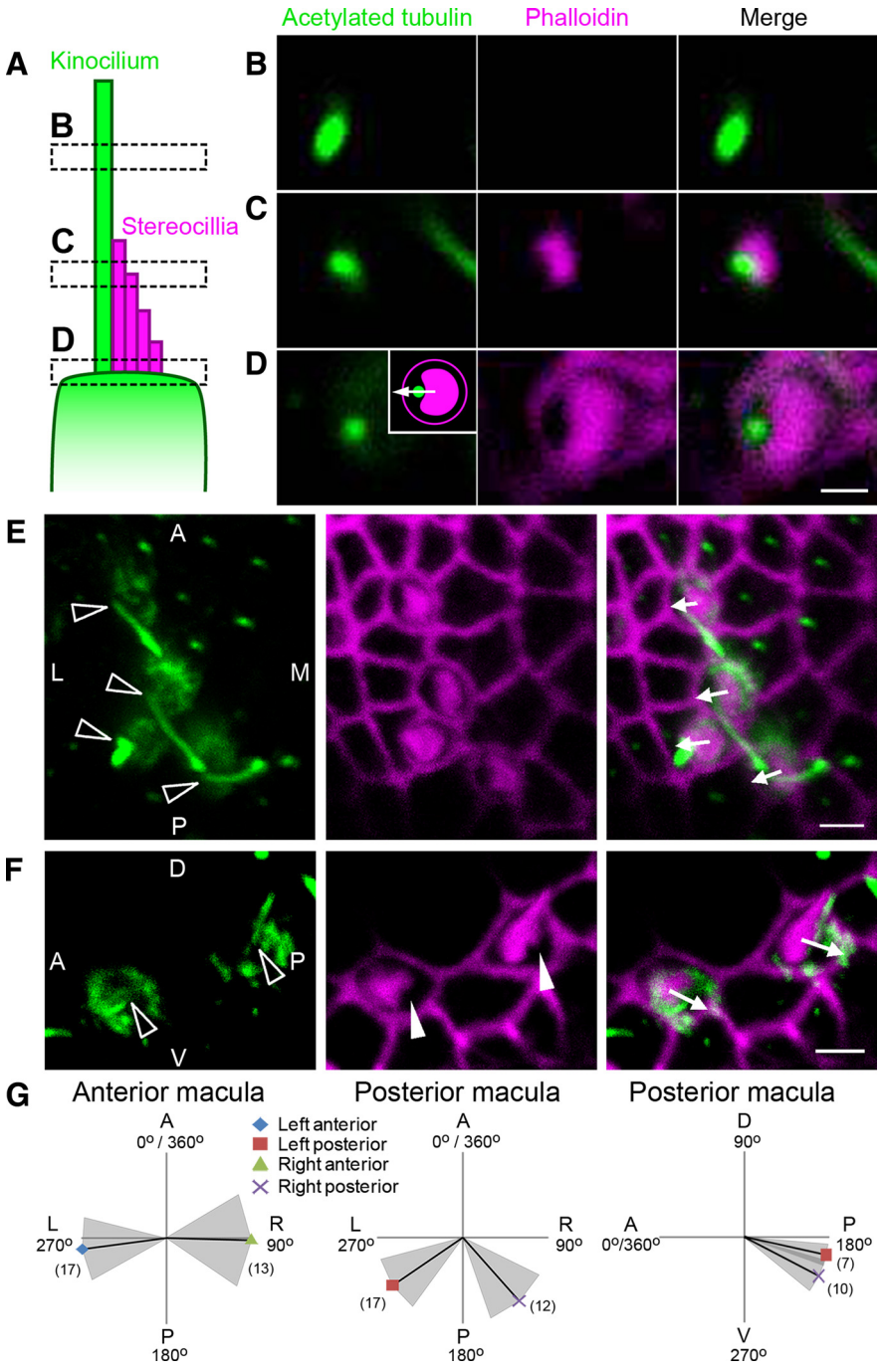

Figure 2. Hair bundles of macular hair cells are unidirectionally arranged at 27 hpf. ***A***, Schematic, side view of a hair cell. Optical sections (dotted squares) are highlighted in ***B–D***. ***B–D***, Top views of the optical slices at upper (***B***), middle (***C***), and basal part (***D***) of the hair bundle that were double-stained with anti-acetylated tubulin antibody (green) and fluorescent phalloidin (magenta). ***B***, Only a single kinocilium (green) was observed in the upper section. ***C***, In the middle, the kinocilium is accompanied by tips of stereocilia (magenta). ***D***, An eccentric arrangement of kinocilium and stereocilia on the apical surface of the hair cell. An arrow indicates the orientation of the hair-bundle polarity in a schema (inset). ***E***, Stacked dorsal image of the anterior macula in the left otic vesicle. An eccentric arrangement of kinocilia (open arrowheads) and stereocilia (magenta) represents the orientation of hair bundles pointing in the lateral direction (arrows). ***F***, Lateral view of the posterior macular hair cells in the left otic vesicle. Open arrowheads represent the base of the kinocilia, where stereocilia are not located (filled arrowheads). The complementary staining indicates the orientation of the hair-bundle polarity pointing in the posteroventral direction (arrows). ***G***, Orientation of hair-bundle polarity of the anterior or posterior macular hair cells. Black lines and gray areas represent mean angles and SDs, respectively. The numbers in parentheses indicate the number of measured cells. Hair-bundle polarity of the anterior macular hair cells was pointing in the lateral direction (left), and that of the posterior macular hair cells was in the posterior-lateral-ventral directions (middle and right). A, P, L, M, D, and V in ***E*** and ***F*** indicate anterior, posterior, lateral, medial, dorsal, and ventral, respectively. Scale bar: (in ***D***) ***B–D***, 1 μm; ***E***, ***F***, 2 μm.

not. The tether cells at 21.5 hpf, however, do not possess stereocilia. To examine whether or not the tether cells acquire stereocilia during the subsequent development, embryos were double-stained with fluorescent-phalloidin and anti-acetylated tubulin antibody.

In the otic vesicle of 20 hpf embryos (Fig. 4*A*,*B*), numerous cilia were labeled with the anti-acetylated-tubulin antibody, as reported previously (Riley et al., 1997). At the anterior and posterior ends, tether cells (usually two per macula) were distinguished from others because their apical cytoplasm was stained positively with the antibody (Fig. 4*B*). The mean number of tether cells in the anterior macula were between two and three during 20–24 hpf (Fig. 4*F*, green bars), and the tether cilia gradually elongated (Fig. 4*G*). In contrast, the number of non-tether ciliary cells dramatically decreased, as described previously (Fig. 4*F*, blue bars) (Riley et al., 1997; Colantonio et al., 2009), although a small number of non-tether cells still retained the cilia (Fig. 4*G*). Fluorescent-phalloidin labeled only superficial actin filaments, and actin-based stereociliary protrusions from the epithelial surface were not evident until 21 hpf (Fig. 4*C*). At 22 hpf, villous labeling with fluorescent-phalloidin was observed on the apical surface of the tether cells (Fig. 4*D*). This became more obvious at 24 hpf (Fig. 4*E*), whereas the phalloidin-positive protrusion never appeared on the non-tether cells. The number of tether cells with stereocilia gradually increased in the anterior macula (Fig. 4*F*, red bars; 1.2 $\pm$ 1.3 at 22 hpf, $n = 5$; 1.8 $\pm$ 1.6 at 23 hpf, $n = 6$; 2.8 $\pm$ 1.0 at 24 hpf, $n = 6$; n represents the number of maculae examined), and the stereocilia gradually extended over time (Fig. 4*G*). Similar results were obtained in the posterior macula (supplemental Fig. S2, available at www.jneurosci.org as supplemental material). It is thus evident that the tether cells obtain stereocilia from 22 hpf and morphologically differentiate into the first hair cells, whereas non-tether cells lose their cilia during the early developmental period.

Acquisition of polarized arrangements of hair bundles in tether cells

The direction of hair-bundle polarity was evaluated from the arrangement of tubulin-based cilia and actin filaments. At the anteroventral part of the otic vesicle, dorsal views of ciliary cells labeled with fluorescent phalloidin revealed an actin meshwork structure at the apical cell–cell boundary, whereas the apex of ciliated

cells was not labeled at 20 hpf (Fig. 5*A*). At 21 hpf, phalloidin staining revealed a medially located, eccentric patch on the tether cells (6 of 14 cells, 6 maculae, Fig. 5*B*), indicating cell polarization, although the phalloidin-positive protrusion from the epithelial surface was not evident (Fig. 4*C*). The eccentric arrangement of cilia and phalloidin staining was evident in all tether cells from 22 hpf, indicating that anterior tether cells possess laterally polarized hair bundles (Fig. 5*C–F*). Similarly, posterior tether cells acquired a polarized arrangement of hair bundles pointing in the posterolateral direction from 23 hpf (Fig. 5*F*; supplemental Fig. S2, available at www.jneurosci.org as supplemental material). These data suggest that the stereocilia of tether cells are already unidirectionally arranged upon initiation of their elongation.

Tether cells acquire mechanotransduction channels at 23 hpf

Mechanoelectrical transduction channels in the hair cells are thought to exist at the tip of stereocilia (Hudspeth, 1982; Jaramillo and Hudspeth, 1991; Beurg et al., 2009). When do tether cells acquire mechanotransduction channels? We assessed this by examining FM1-43 incorporation into the tether cells. Differential interference contrast (DIC) images of the anteroventral part of the otic vesicle at 22 hpf revealed cilia attached to the otolith (Fig. 6*A*,*B*). Judging from their locations and the fact that the cilia were associated with the otolith, the ciliated cells were identified as tether cells. The tether cells, however, were never labeled with the dye before 22 hpf (9 fish). At 23 hpf, the fluorophore selectively permeated the tether cells (Fig. 6*C*,*D*). In Figure 6*C*, a single tether cilium (filled arrowheads) was associated with a trapezoidal structure (open arrowheads) on the epithelium; these correspond to a single kinocilium and a bundle of stereocilia, respectively. At 24 hpf, a single kinocilium coupled to the otolith (Fig. 6*E*, filled arrowheads) and a triangular stereocilia (Fig. 6*E*, arrows) were clearly observed. Otolithic membrane was not evident at the early developmental stage. The number of labeled cells in the anterior macula (Fig. 6*G*; 1.5 ± 1.0 at 23 hpf, $n = 6$; 2.2 ± 0.4 at 24 hpf, $n = 5$; 2.5 ± 0.8 at 27 hpf, $n = 6$, n represents the number of fish examined) were comparable to that of tether cells with stereocilia (Fig. 4*F*), suggesting that all the cells with hair bundles took up the dye from 23 hpf. Posterior tether cells were also labeled with the fluorescent marker from 23 hpf (supplemental Fig. S3, available at www.jneurosci.org as supplemental material). These observations suggest that tether cells on anterior and posterior macula acquire mechanotransduction channels at 23 hpf, raising the possibility that the tether cells permeate ions intracellularly by gating the mechanotransduction channels.

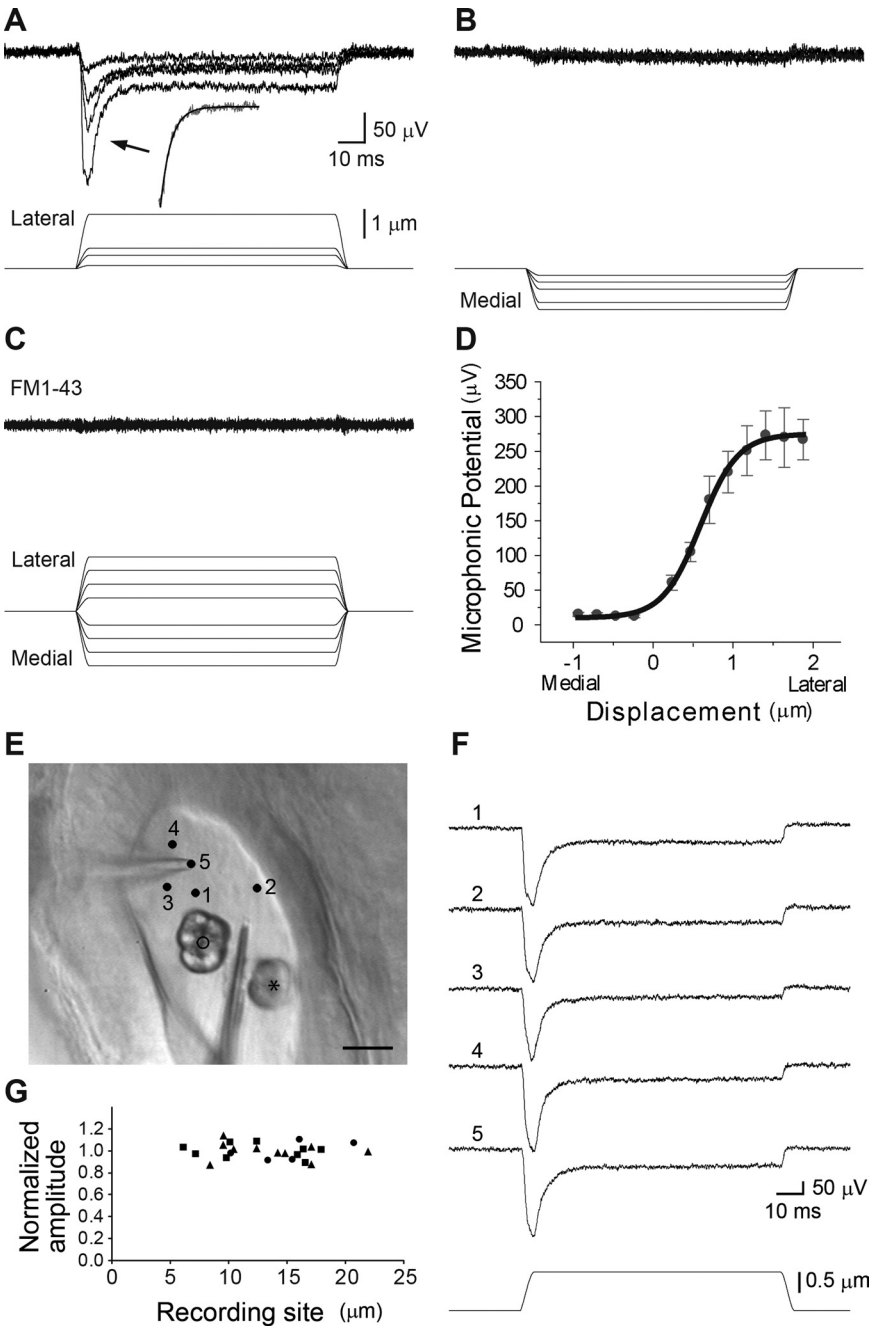

Figure 3. Electrophysiological properties of microphonic potentials at 27 hpf. ***A***, Microphonic potentials (upper traces) elicited by displacement of the anterior otolith in the lateral direction (lower traces). A transient, negative potential was followed by a sustained component. The decay phase of the response (arrow) was fitted by a first-order exponential function. The stimulus monitor is the driver voltage that was calibrated to step size (see supplemental Fig. S1, available at www.jneurosci.org as supplemental material). Scale bars also apply to the inset trace (***B***, ***C***). ***B***, Remarkable responses were not elicited by otolith displacement in the medial direction. ***C***, Responses were suppressed by a mechanotransduction blocker, FM1-43, which was injected into the otic vesicle. ***D***, Mean peak amplitudes from 8 fish (mean ± SEM) were plotted against displacement of the otolith and fit with a Boltzmann equation. ***E***, Filled circles with numbers indicate various recording sites in the dorsal-view photograph. A recording pipette (left) marks one of the recording positions. The center of the anterior otolith was marked with an open circle. Posterior otolith (asterisk) was removed from the posterior macula using a stimulus probe (bottom) (see Materials and Methods). Anterior is up, and lateral is left. Scale bar, 10 μm. ***F***, Microphonic potentials, recorded at the locations shown in ***E***, exhibited similar waveforms. ***G***, Anti-peak amplitudes of individual traces were normalized to the mean values, and plotted against distances from the center of the otolith (open circle in ***E***) for each recording site ($n = 24$, 3 fish). All traces shown are averaged waveforms from 40 consecutive sweeps.

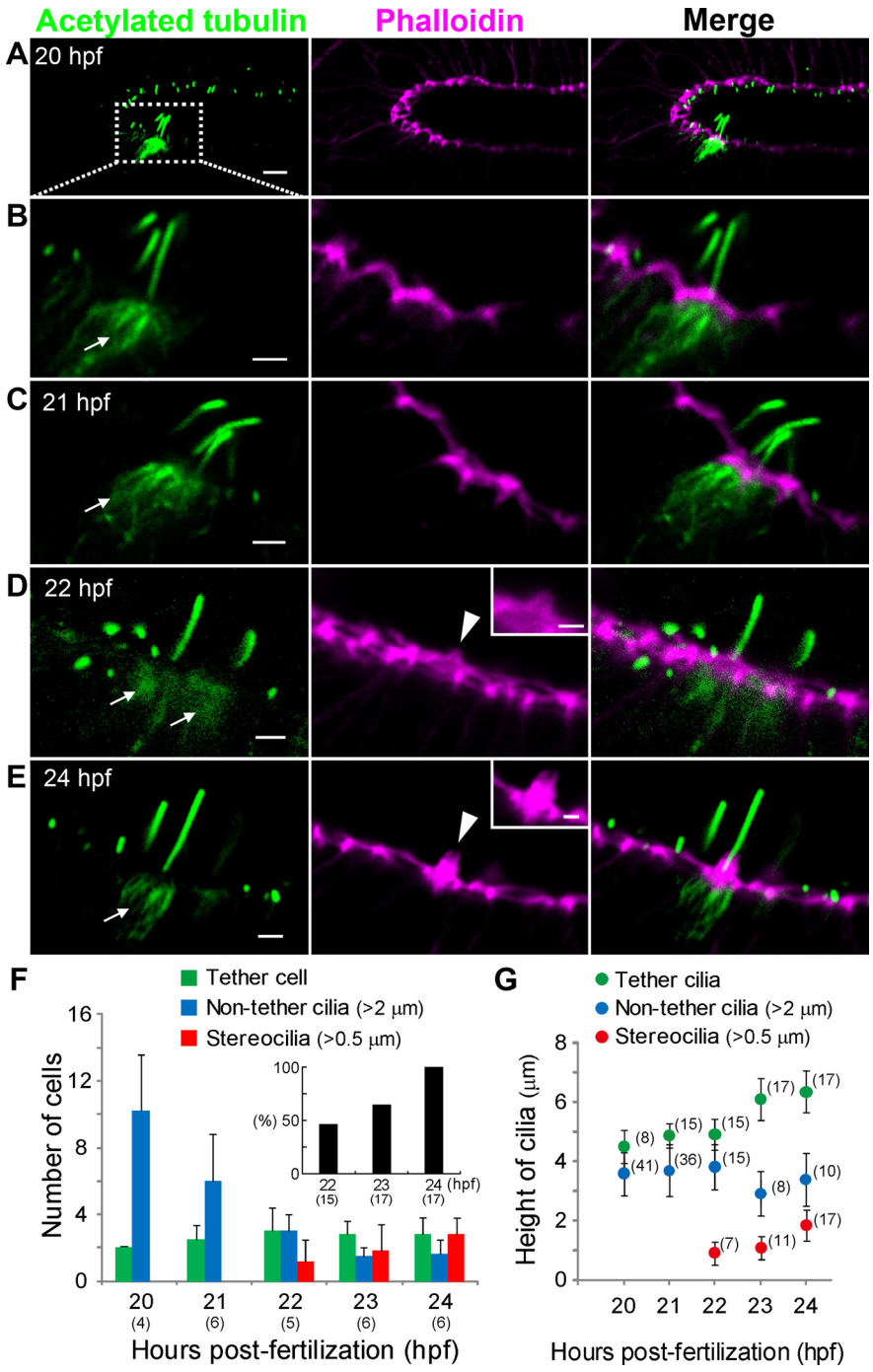

Figure 4. Acquisition of stereociliary bundles in tether cells. ***A–E***, Lateral views of the otic vesicle. Embryos were stained at 20–24 hpf with anti-acetylated tubulin antibody (green) and fluorescent phalloidin (magenta). ***A***, Numerous cilia were labeled with anti-acetylated tubulin antibody at 20 hpf. Cortical actin meshwork was stained with fluorescent phalloidin. Dotted square in ***A*** is highlighted in ***B***. ***B–E***, Enlarged images of the anteroventral part of the otic vesicle, as indicated by a dotted square in ***A***. ***B***, ***C***, At 20–21 hpf, ciliated cells were immunoreactive with the anti-acetylated tubulin antibody at their apical somata (arrows); these cells were identified as tether cells. No obvious protrusions were labeled with fluorescent phalloidin. ***D***, At 22 hpf, a triangular protrusion (arrowhead and inset) on tether cells (arrows) was positively labeled with fluorescent phalloidin. ***E***, At 24 hpf, phalloidin obviously stained a hair-bundle-like structure (arrowhead and inset) on a tether cell (arrow). Anterior is to the left, and dorsal is up in all images. Scale bars: ***A***, 5 μm; ***B–E***, 2 μm; insets in ***D*** and ***E***, 1 μm. ***F***, The number of ciliated cells at the anteroventral part of the otic vesicle (mean ± SD). Green, blue, and red bars indicate the number of tether cells, non-tether cells with long cilium (>2 μm), and cells with stereocilia (>0.5 μm), respectively. The number of non-tether ciliated cells decreased during 20–24 hpf, whereas the number of tether cells appeared to be constant. Stereocilia appeared at 22 hpf. The numbers in parentheses indicate the number of the anterior macula examined. Inset graph shows the proportion of the tether cells with stereocilia (>0.5 μm) to the total tether cells. The numbers in parentheses are the number of tether cells analyzed. ***G***, The length of tether-cell cilia, non-tether-cell cilia, and stereocilia in tether cells (mean ± SD). Tether-cell cilia and stereocilia gradually extended during 20–24 hpf, whereas the mean height of non-tether cilia did not increase. The numbers in parentheses indicate the number of cells.

Acquisition of mechanoelectrical transduction responses in tether cells

To directly examine when the tether cells acquire mechanosensitivity, microphonic potentials in response to otolith displacement were recorded in the otic vesicle of embryos at 22–24 hpf. Displacement of the anterior otolith in any direction never evoked obvious responses until 22 hpf (Fig. 7*A*, 4 fish). A microphonic potential was first observed at 23 hpf; lateral displacement of the anterior otolith elicited a transient negative potential that adapted over ~10 ms (Fig. 7*B*, 4 fish). Medial displacement of the otolith, however, did not evoke obvious responses, suggesting that the tether cells already have directional selectivity to mechanical stimulus, as indicated by the laterally polarized arrangement of hair bundles (Fig. 5). Microphonic potentials became more obvious with an increase in the amplitude at 24 hpf (Fig. 7*C*, 3 fish). The decay time course of the transient potential was fit by a single-order exponential function with time constants of 6.6 ± 3.2 ms at 23 hpf (4 fish) and 6.2 ± 2.8 ms at 24 hpf (3 fish) (step size ~0.5 μm). These microphonic potentials were blocked by FM1-43 (Gale et al., 2001), injected into the otic vesicle (Fig. 7*B*,*C*; 2 fish at 23 hpf; 2 fish at 24 hpf). Previous studies have shown that the developing otolith spontaneously oscillates at the frequency of 34 Hz due to the motile cilia (Riley et al., 1997; Colantonio et al., 2009), but the spontaneous activity was not observed in the comparison between the microphonic potentials with and without FM1-43. Figure 7*D* shows a developmental enhancement in the response-displacement relationship in the early stages. Similar results were obtained from the recordings of microphonic potentials of posterior macular hair cells (supplemental Fig. S4, available at www.jneurosci.org as supplemental material). These data demonstrate that hair cells acquire direction-selective mechanosensitivity at 23 hpf, thus suggesting that tether cells differentiate into the first functional sensory hair cells.

Discussion

Morphological and functional differentiation from tether cells into the first hair cells in zebrafish inner ear

Previous morphological observations in zebrafish embryos suggested that tether cells, ciliary cells at the anterior and posterior ends of the otic vesicle, are premature hair cells (Haddon and Lewis, 1996; Riley et al., 1997). However, neither the appearance of stereocilia in tether cells nor the acquisition of mechanosensitivity has been clarified. The present immunohis-

tochemical study revealed that tether cells acquire actin-based stereociliary bundles at 22 hpf, whereas stereocilia do not appear in non-tether cells (Fig. 4). In addition, *in vivo* labeling with FM1-43 suggested that mechanotransduction channels are localized on tether cells from 23 hpf (Fig. 6). Furthermore, microphonic potentials obtained in the otic vesicle revealed that tether cells acquire direction-selective mechanosensitivity with an adaptation mechanism at 23 hpf (Fig. 7). Hence, these morphological and electrophysiological analyses directly demonstrated that tether cells become the first functional hair cells in the zebrafish inner ear.

Early acquisition of hair-bundle polarity

The orientational arrangement of the hair bundle is an important hallmark of inner ear hair cells in vertebrates. In mice, utricular and saccular hair bundles first appear on the apical surface of differentiating hair cells at embryonic day 13.5 (E13.5) (Denman-Johnson and Forge, 1999). The hair cells are initially not polarized. A kinocilium is located at the center of the cell surface and is surrounded by short microvilli of the same length. The staircase-like pattern of hair bundles is established as the kinocilium becomes eccentrically positioned. Similar stepwise establishment of hair-bundle polarization has been demonstrated in chicken and rodent cochlear hair cells (Tilney et al., 1992; Zine and Romand, 1996). In zebrafish, however, hair-bundle polarity is already established at 22 hpf when the stereocilia begin to extend (Fig. 5); the hair-bundle orientation is similar to that observed at 30 hpf (Haddon et al., 1999). Thus, mechanisms underlying the polarization of the hair bundles may already function in zebrafish tether cells by the onset of the stereocilia extension.

It has been hypothesized that, in birds and mammals, directional growth of the extracellular matrix, such as the tectorial membrane in the cochlea and the otolithic (or otoconial) membrane in the maculae, determines hair-bundle polarity (Cotanche and Corwin, 1991). The otoconial membrane in mice, however, is formed simultaneously across the macula and does not exhibit obvious bias of matrix synthesis (Denman-Johnson and Forge, 1999). In addition, the orientation of cochlear hair cell bundles becomes evident before the tectorial membrane is formed (Lim and Anniko, 1985). Furthermore, the otolithic membrane is not evident in zebrafish embryos at the time of formation of

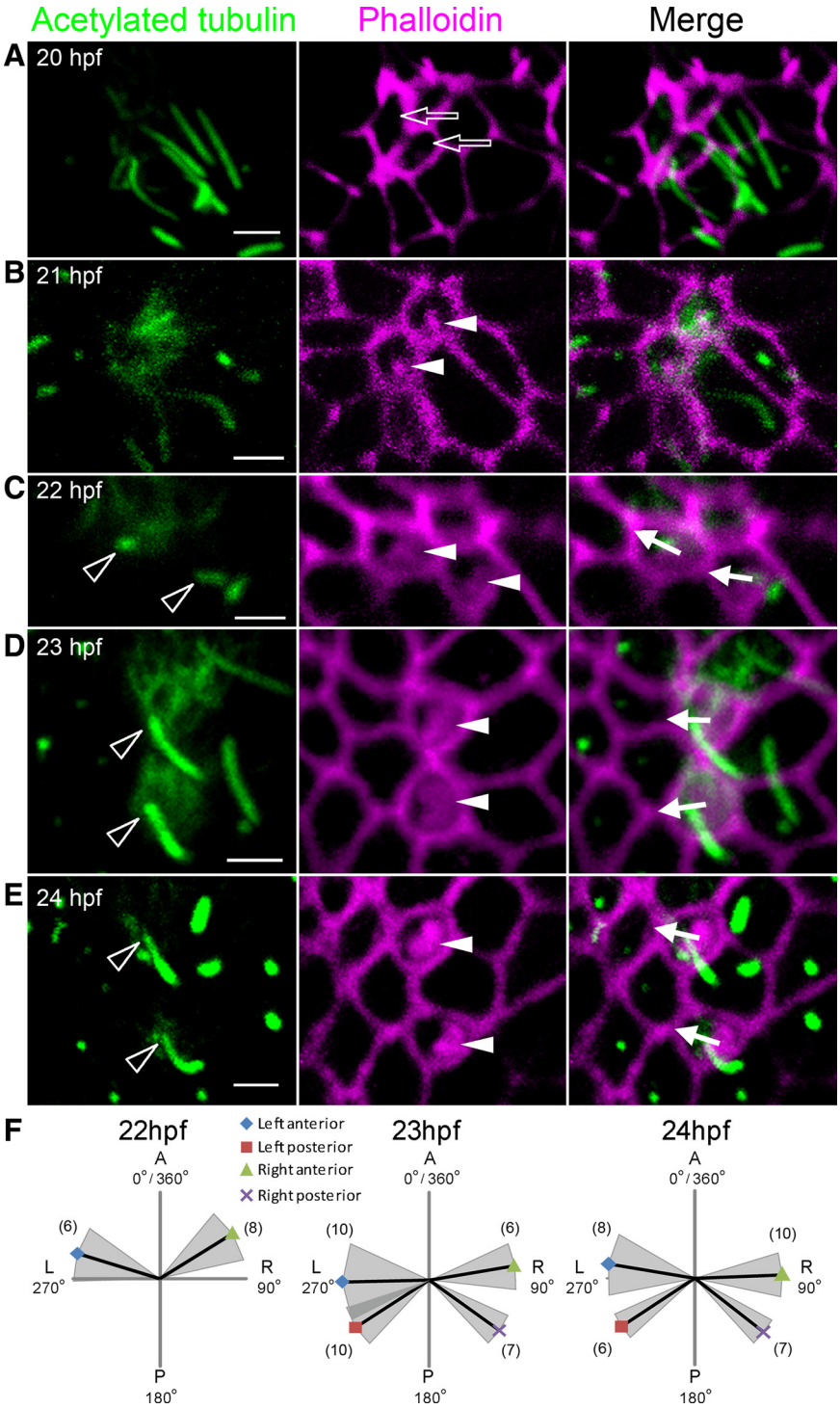

Figure 5. Acquisition of hair-bundle polarity in tether cells. ***A–E***, Top views of ciliated cells at the anteroventral part of the left otic vesicle stained with anti-acetylated tubulin antibody (green) and fluorescent phalloidin (magenta) at 20–24 hpf. Anterior is up, and lateral is to the left in all of the figures. Scale bar: ***A***, 2 μm. At 20 hpf, several cilia were labeled with anti-acetylated tubulin antibody. Fluorescent phalloidin labeled the cortical actin meshwork, but no obvious structure was evident on the apex of the tether cells (open arrows). ***B***, At 21 hpf, eccentric patches on the surface were stained with fluorescent phalloidin (filled arrowheads, 6 of 14 tether cells, 6 maculae). ***C–E***, From 22 hpf, the eccentric arrangement of the base of tether-cell cilia (open arrowheads) and phalloidin-positive patches (filled arrowheads) became evident in all tether cells, and indicated hair-bundle polarity pointing in the lateral direction (arrows). ***F***, Orientation of hair-cell polarity during 22–24 hpf [mean (black lines) ± SD (gray areas)]. The numbers in parentheses indicate the number of measured cells. Anterior tether cells acquire their polarities oriented in the lateral directions by 22 hpf, and posterior tether cells obtained posterolateral polarity by 23 hpf.

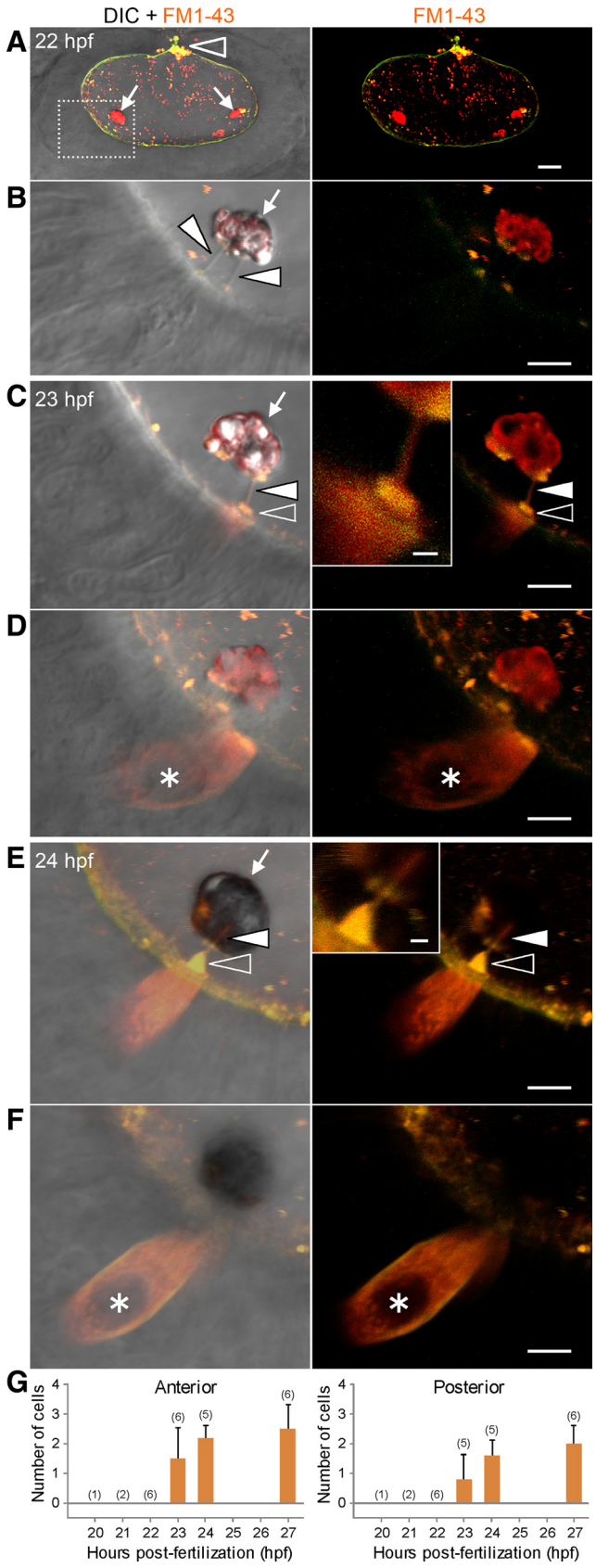

Figure 6. Tether cells begin to take up FM1-43 at 23 hpf. ***A***, Z-series stack of images of the otic vesicle viewed laterally at 22 hpf under DIC optics. FM1-43 was injected into the lumen with a micropipette inserted through the dorsal epithelium (arrowhead). Arrows indicate the anterior and posterior otoliths. Otolith surfaces and numerous otolith precursors inside the lumen were labeled with FM1-43, showing successful injection of the dye. The dotted square in ***A*** is highlighted in ***B***. ***B***, Two cilia (filled arrowheads) tethering the otolith (arrow) were present in the DIC image, whereas no cells incorporated the fluorophore. ***C–F***, Anteroventral part of the otic vesicle at 23 hpf (***C***, ***D***) and 24 hpf (E, F). Cilia and somata of tether cells were labeled with FM1-43 from 23 hpf. ***C***, A single tether-cell cilium (filled arrowhead) coupled to the otolith (arrow) and the trapezoidal structure (open arrowhead) were labeled (inset). ***D***, In a stacked image focused on the basal part of the same cell in ***C***, the dye filled the cytoplasm of the tether cell, but was excluded from the nucleus (asterisk). ***E***, A tether cell was labeled with FM1-43. A single tether cilium (filled arrowhead) associated with a triangular structure (open arrowhead) was present on the apex (inset). ***F***, The fluorophore permeated into the cytoplasm of the same tether cell in ***E***. Anterior is to the left, and dorsal is up. Scale bars: ***A***, 10 μm; ***B–F***, 5 μm; insets in ***C***, ***E***, 1 μm. ***G***, The number of cells labeled with FM1-43 at each stage (mean ± SD). The numbers in parentheses indicate the number of fish examined. For both anterior and posterior macula, FM1-43 uptake begins at 23 hpf.

hair-bundle orientation; it appears by 7 d postfertilization (Hughes et al., 2004). Thus, directional growth of the extracellular matrix is unlikely to be a key factor in determining hair-bundle polarity.

Alternatively, several lines of evidence have shown that hair-bundle orientation in mammalian inner ear sensory organ is organized by the planar cell polarity (PCP) signaling pathway (for review, see Chacon-Heszele and Chen, 2009). PCP proteins including Van Gogh-like 2 (Vangl2) (Montcouquiol et al., 2006), Frizzled 3 (Fz3) and Fz6 (Wang et al., 2006), Disheveled 2 (Dvl2) and Dvl3 (Wang et al., 2005; Etheridge et al., 2008), and Prickle-like 2 (Pk2) (Deans et al., 2007) asymmetrically localize along the mediolateral axis in the sensory epithelium. Mutations in PCP genes result in misorientation of hair bundles in the inner ear, whereas formation of polarized hair bundles in each hair cell does not appear to be affected (Curtin et al., 2003; Montcouquiol et al., 2003; Wang et al., 2005; Wang et al., 2006; Qian et al., 2007).

In addition, ablation of kinocilia by knocking out genes that is required for cilia formation results in misoriented hair bundles in mice, whereas asymmetric localization of PCP proteins is not affected by ciliary dysfunction, indicating that kinocilia are necessary for hair cell polarization (Jones et al., 2008). The misorganized hair bundle orientation in the ciliary mutants remarkably correlated with the basal body positioning. These evidence suggest that cilia and basal body have a role downstream of membrane-associated PCP protein complexes in determining the intrinsic polarity of hair cells. Although the machinery for the hair bundle polarization has not been extensively investigated in zebrafish, the amenability of embryos and larvae to genetic dissection and *in vivo* imaging will further clarify the molecular mechanisms underlying the establishment of hair-bundle polarity in the vertebrate inner ear.

Developmental acquisition of mechanosensitivity in tether cells

The acquisition of mechanotransduction in developing hair cells has been studied in dissociated hair cells or isolated maculae and cochleae in chicken and rodents. In the mouse utricle, for instance, the tip links interconnecting stereociliary bundles (Gillespie and Müller, 2009; Sakaguchi et al., 2009) appear between E15 and E17, a few days after the appearance of hair bundles (Denman-Johnson and Forge, 1999; Géléoc and Holt, 2003). Concurrently, hair cells begin to take up FM1-43 and exhibit mechanotransducer currents between E16 and E17 (Géléoc and Holt, 2003). Chicken and mice cochlear hair cells follow the same sequence (Si et al., 2003; Waguespack et al., 2007; Lelli et al., 2009).

The present physiological analysis of the mechanosensitivity of macular hair cells, performed *in vivo* in zebrafish embryos,

demonstrated that mechanotransduction occurred concurrently with FM1-43 uptake by tether cell at 23 hpf (Figs. 6, 7), within an hour after the beginning of stereociliary growth (22 hpf, Fig. 4). Previous studies on the expression of tip-link components (Kazmierczak et al., 2007; Lelli et al., 2010), *cadherin 23* (*cdh23*) and *protocadherin 15* (*pcdh15*), indicate that the tip links appear on tether cells by 24 hpf (Söllner et al., 2004; Seiler et al., 2005). Moreover, in mutant zebrafish with defects in the tip-link genes, hair cells exhibit sprouting bundles and lack both FM1-43 incorporation and microphonic potentials, resulting in hearing loss and vestibular dysfunction (Nicolson et al., 1998; Seiler and Nicolson, 1999; Siemens et al., 2004; Söllner et al., 2004; Seiler et al., 2005). Therefore, it is most likely that tip links connect adjacent stereociliary tips by 23 hpf. Together, the mechanotransduction apparatus in zebrafish is assembled and becomes functional within an hour after the beginning of stereocilia extension.

The rapid acquisition of mechanosensitivity in tether cells is similar to that in mouse vestibular hair cells, where mechanotransducer currents rapidly mature during E16 (Géléoc and Holt, 2003). Cochlear hair cells in chicken and mice, in contrast, gradually develop their mechanotransduction properties over several days from the appearance of the responses (Si et al., 2003; Waguespack et al., 2007; Lelli et al., 2009). Thus, the process of functional maturation of macular hair cells may be different from that of cochlear hair cells (Géléoc and Holt, 2003; Lelli et al., 2009). The onset of mechanotransduction in zebrafish is ~20 h before the acquisition of auditory responsiveness (Tanimoto et al., 2009). The early acquisition of hair-cell mechanotransduction before the onset of hearing corresponds to the evidence in chicken and rodents (Kennedy et al., 2003; Si et al., 2003; Lelli et al., 2009).

The microphonic potentials developed during hours following the appearance of the response at 23 hpf (Figs. 3*D*, 7D). Because the potentials represent the total current flow of mechanotransduction in the otic vesicle, as indicated in Figure 3, *E*–G, the developmental enhancement can be explained by the increase in the number of functional hair cells and/or the upregulation of functional mechanotransduction channels in each hair cell. The latter possibility is likely because the number of hair cells labeled with FM1-43 does not change between 23 hpf and 27 hpf (Fig. 6*G*), whereas the amplitude of the microphonic potential increased remarkably (Figs. 3, 7).

The stimulus with a slow rise time of 5 ms was used in this study (see Materials and Methods), which may make us underestimate the peak amplitude and overestimate the time constant of the response, since with the slower stimulus onsets, response magnitude is reduced and the adaptation is slowed in a previous study (Wu et al., 1999). Therefore, given that the stimulus with a faster rise time of 0.1 ms, the amplitude can be estimated to be approximately two times larger and the adaptation time constant is more than three times faster than those obtained in the present study.

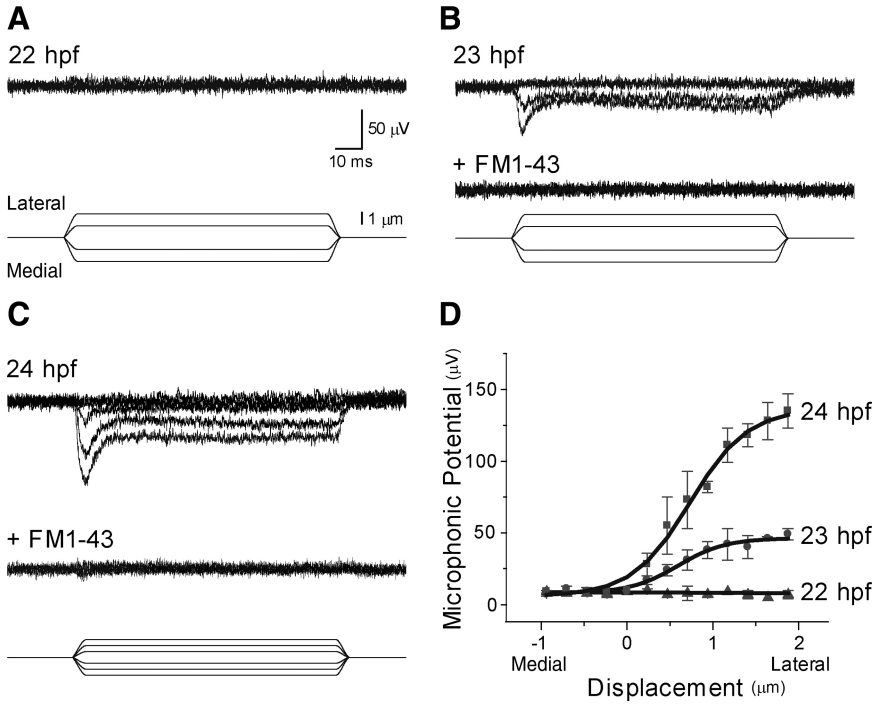

Figure 7. Tether cells acquire mechanosensitivity at 23 hpf. ***A–C***, Microphonic potentials (upper traces) recorded in embryos at 22 hpf (***A***), 23 hpf (***B***), and 24 hpf (***C***) in response to displacement of the anterior otolith (lower traces). All traces shown are averaged waveforms from 40 consecutive sweeps. The stimulus driver voltage was indicated in lower traces as in Figure 3. Scale bars in ***A*** also apply to ***B*** and ***C***. ***A***, Obvious responses were not elicited by otolith displacement at 22 hpf. ***B***, At 23 hpf, movement of the otolith toward the lateral side evoked negative potentials that adapted over ~10 ms, whereas medial movement did not induce responses. The responses were suppressed by a mechanotransduction blocker, FM1-43, injected into the otic vesicle. ***C***, Microphonic potentials became larger at 24 hpf, which were again blocked with FM1-43. ***D***, Peak amplitude (mean ± SEM, 3–4 fish) was plotted against displacement of the otolith and fit with a Boltzmann equation (10–90% operating ranges, 1.3 μm at 23 hpf and 1.4 μm at 24 hpf; resting open probability, 11.1% at 23 hpf and 8.5% at 24 hpf).

It has been shown that microphonic potentials exhibit rebound or off responses to step displacement and responses to negative deflection (Corey and Hudspeth, 1983a,b), but not observed in the present study. This difference may be explained by three reasons; first, immaturity of hair cells as in previous studies, in which the developing hair cells in chicken or mice exhibit little or no rebound and off responses to step displacement (Géléoc and Holt, 2003; Kennedy et al., 2003; Lelli et al., 2009). Second, ionic environment affects the microphonic responses; it has been shown that high apical extracellular Ca^{2+} decreases the amplitude of the responses and blocks responses to negative displacement (Corey and Hudspeth, 1983b). Finally, the absence of those responses in this study may be due to a technical reason; the recording of the extracellular microphonic potentials from two hair cells has a difficulty in obtaining high signal-to-noise ratio. The rebound or off response might be hidden by the baseline noise. These possibilities as well as spontaneous activity due to the motile cilia should be examined in further studies through the whole-cell recording from the hair cells.

Tether cells as the origin of sensory hair cells

The origin of vertebrate hair cells has been discussed by comparing their morphology and genetic properties to those of invertebrate mechanosensory cells. The apical specialization of invertebrate mechanosensory cells contrasts with the staircase-like arrangement of actin-based stereocilia associated with a single kinocilium in vertebrate hair cells (Fritzsch et al., 2006, 2007).

In arthropods, for example, mechanoreceptors in chordotonal organs possess a single cilium without actin-based microvilli (Caldwell and Eberl, 2002), although there are some exceptions (e.g., hair cells with a directional collar of microvilli in jellyfish and ascidians (Arkett et al., 1988; Manni et al., 2004)). It should be noted that, before 22 hpf, tether cells possess a single cilium without stereocilia like invertebrate mechanosensory cells, but subsequently, tether cells acquire an orientational arrangement of stereociliary bundles, forming into vertebrate inner ear hair cells (Fig. 4).

In contrast to the morphological differences between vertebrate hair cells and invertebrate mechanoreceptor cells, a common genetic mechanism plays a central role in their formation (Fritzsch and Beisel, 2001; Caldwell and Eberl, 2002). In *Drosophila*, for instance, a proneural gene, *atonal*, is critical for the differentiation of the chordotonal organ, including ciliated mechanosensory neurons (Jarman et al., 1993; for review, see Furman and Bukharina, 2008). Expression of a mouse *atonal* homolog, *atoh1*, is required for the genesis of hair cells in mice (Bermingham et al., 1999). Again in zebrafish, an *atonal* homolog, *atoh1b*, is expressed at the anterior and posterior ends of the otic vesicles by 14 hpf and is necessary for the differentiation of tether cells (Millimaki et al., 2007). Thus, zebrafish tether cells, mammalian hair cells and invertebrate mechanosensory cells may have a common developmental genetic origin (for review, see Caldwell and Eberl, 2002). The morphological and functional differentiation from ciliary cells to hair cells in zebrafish embryos may recapitulate the evolutionary transition from ancestral ciliated cells to vertebrate inner ear hair cells.

The present analysis demonstrates that tether cells acquire an orientational arrangement of stereociliary bundles and direction-selective mechanosensitivity by 23 hpf, and they therefore morphologically and functionally differentiate into the first sensory hair cells in the zebrafish inner ear. On the basis of the morphological analysis and the *in vivo* electrophysiological recording techniques described herein, together with the amenability of embryonic zebrafish to genetic manipulation, it will be possible to further clarify the molecular basis of hair-bundle formation and mechanotransduction in vertebrate inner ear hair cells.

References

Arkett SA, Mackie GO, Meech RW (1988) Hair cell mechanoreception in the jellyfish *Aglantha digitale*. J Exp Biol 135:329–342.

Bermingham NA, Hassan BA, Price SD, Vollrath MA, Ben-Arie N, Eatock RA, Bellen HJ, Lysakowski A, Zoghbi HY (1999) Math1: an essential gene for the generation of inner ear hair cells. Science 284:1837–1841.

Beurg M, Fettiplace R, Nam JH, Ricci AJ (2009) Localization of inner hair cell mechanotransducer channels using high-speed calcium imaging. Nat Neurosci 12:553–558.

Caldwell JC, Eberl DF (2002) Towards a molecular understanding of *Drosophila* hearing. J Neurobiol 53:172–189.

Chacon-Heszele MF, Chen P (2009) Mouse models for dissecting vertebrate planar cell polarity signaling in the inner ear. Brain Res 1277:130–140.

Colantonio JR, Vermot J, Wu D, Langenbacher AD, Fraser S, Chen JN, Hill KL (2009) The dynein regulatory complex is required for ciliary motility and otolith biogenesis in the inner ear. Nature 457:205–209.

Corey DP, Hudspeth AJ (1983a) Analysis of the microphonic potential of the bullfrog's sacculus. J Neurosci 3:942–961.

Corey DP, Hudspeth AJ (1983b) Kinetics of the receptor current in bullfrog saccular hair cells. J Neurosci 3:962–976.

Corey DP, García-Añoveros J, Holt JR, Kwan KY, Lin SY, Vollrath MA, Amalfitano A, Cheung EL, Derfler BH, Duggan A, Géléoc GS, Gray PA, Hoffman MP, Rehm HL, Tamasauskas D, Zhang DS (2004) TRPA1 is a candidate for the mechanosensitive transduction channel of vertebrate hair cells. Nature 432:723–730.

Cotanche DA, Corwin JT (1991) Stereociliary bundles reorient during hair cell development and regeneration in the chick cochlea. Hear Res 52:379–402.

Curtin JA, Quint E, Tsipouri V, Arkell RM, Cattanach B, Copp AJ, Henderson DJ, Spurr N, Stanier P, Fisher EM, Nolan PM, Steel KP, Brown SD, Gray IC, Murdoch JN (2003) Mutation of Celsr1 disrupts planar polarity of inner ear hair cells and causes severe neural tube defects in the mouse. Curr Biol 13:1129–1133.

Deans MR, Antic D, Suyama K, Scott MP, Axelrod JD, Goodrich LV (2007) Asymmetric distribution of prickle-like 2 reveals an early underlying polarization of vestibular sensory epithelia in the inner ear. J Neurosci 27:3139–3147.

Denman-Johnson K, Forge A (1999) Establishment of hair bundle polarity and orientation in the developing vestibular system of the mouse. J Neurocytol 28:821–835.

Etheridge SL, Ray S, Li S, Hamblet NS, Lijam N, Tsang M, Greer J, Kardos N, Wang J, Sussman DJ, Chen P, Wynshaw-Boris A (2008) Murine dishevelled 3 functions in redundant pathways with dishevelled 1 and 2 in normal cardiac outflow tract, cochlea, and neural tube development. PLoS Genet 4:e1000259.

Fritzsch B, Beisel KW (2001) Evolution and development of the vertebrate ear. Brain Res Bull 55:711–721.

Fritzsch B, Pauley S, Beisel KW (2006) Cells, molecules and morphogenesis: the making of the vertebrate ear. Brain Res 1091:151–171.

Fritzsch B, Beisel KW, Pauley S, Soukup G (2007) Molecular evolution of the vertebrate mechanosensory cell and ear. Int J Dev Biol 51:663–678.

Furman DP, Bukharina TA (2008) How *Drosophila melanogaster* forms its mechanoreceptors. Curr Genomics 9:312–323.

Gale JE, Marcotti W, Kennedy HJ, Kros CJ, Richardson GP (2001) FM1-43 dye behaves as a permeant blocker of the hair-cell mechanotransducer channel. J Neurosci 21:7013–7025.

Géléoc GS, Holt JR (2003) Developmental acquisition of sensory transduction in hair cells of the mouse inner ear. Nat Neurosci 6:1019–1020.

Gillespie PG, Müller U (2009) Mechanotransduction by hair cells: models, molecules, and mechanisms. Cell 139:33–44.

Haddon C, Lewis J (1996) Early ear development in the embryo of the zebrafish, *Danio rerio*. J Comp Neurol 365:113–128.

Haddon C, Mowbray C, Whitfield T, Jones D, Gschmeissner S, Lewis J (1999) Hair cells without supporting cells: further studies in the ear of the zebrafish mind bomb mutant. J Neurocytol 28:837–850.

Hanneman E, Westerfield M (1989) Early expression of acetylcholinesterase activity in functionally distinct neurons of the zebrafish. J Comp Neurol 284:350–361.

Hudspeth AJ (1982) Extracellular current flow and the site of transduction by vertebrate hair cells. J Neurosci 2:1–10.

Hudspeth AJ (1989) How the ear's works work. Nature 341:397–404.

Hudspeth AJ, Jacobs R (1979) Stereocilia mediate transduction in vertebrate hair cells (auditory system/cilium/vestibular system). Proc Natl Acad Sci U S A 76:1506–1509.

Hughes I, Blasiole B, Huss D, Warchol ME, Rath NP, Hurle B, Ignatova E, Dickman JD, Thalmann R, Levenson R, Ornitz DM (2004) Otopetrin 1 is required for otolith formation in the zebrafish *Danio rerio*. Dev Biol 276:391–402.

Jaramillo F, Hudspeth AJ (1991) Localization of the hair cell's transduction channels at the hair bundle's top by iontophoretic application of a channel blocker. Neuron 7:409–420.

Jarman AP, Grau Y, Jan LY, Jan YN (1993) atonal is a proneural gene that directs chordotonal organ formation in the *Drosophila* peripheral nervous system. Cell 73:1307–1321.

Jones C, Roper VC, Foucher I, Qian D, Banizs B, Petit C, Yoder BK, Chen P (2008) Ciliary proteins link basal body polarization to planar cell polarity regulation. Nat Genet 40:69–77.

Kazmierczak P, Sakaguchi H, Tokita J, Wilson-Kubalek EM, Milligan RA, Müller U, Kachar B (2007) Cadherin 23 and protocadherin 15 interact to form tip-link filaments in sensory hair cells. Nature 449:87–91.

Kennedy HJ, Evans MG, Crawford AC, Fettiplace R (2003) Fast adaptation of mechanoelectrical transducer channels in mammalian cochlear hair cells. Nat Neurosci 6:832–836.

Kimmel CB, Ballard WW, Kimmel SR, Ullmann B, Schilling TF (1995) Stages of embryonic development of the zebrafish. Dev Dyn 203:253–310.

Lelli A, Asai Y, Forge A, Holt JR, Géléoc GS (2009) Tonotopic gradient in the developmental acquisition of sensory transduction in outer hair cells of the mouse cochlea. J Neurophysiol 101:2961–2973.

Lelli A, Kazmierczak P, Kawashima Y, Müller U, Holt JR (2010) Development and regeneration of sensory transduction in auditory hair cells requires functional interaction between cadherin-23 and protocadherin-15. J Neurosci 30:11259–11269.

Lim DJ, Anniko M (1985) Developmental morphology of the mouse inner ear. A scanning electron microscopic observation. Acta Otolaryngol Suppl 422:1–69.

Manni L, Caicci F, Gasparini F, Zaniolo G, Burighel P (2004) Hair cells in ascidians and the evolution of lateral line placodes. Evol Dev 6:379–381.

Meyers JR, MacDonald RB, Duggan A, Lenzi D, Standaert DG, Corwin JT, Corey DP (2003) Lighting up the senses: FM1-43 loading of sensory cells through nonselective ion channels. J Neurosci 23:4054–4065.

Millimaki BB, Sweet EM, Dhason MS, Riley BB (2007) Zebrafish atoh1 genes: classic proneural activity in the inner ear and regulation by Fgf and Notch. Development 134:295–305.

Montcouquiol M, Rachel RA, Lanford PJ, Copeland NG, Jenkins NA, Kelley MW (2003) Identification of Vangl2 and Scrb1 as planar polarity genes in mammals. Nature 423:173–177.

Montcouquiol M, Sans N, Huss D, Kach J, Dickman JD, Forge A, Rachel RA, Copeland NG, Jenkins NA, Bogani D, Murdoch J, Warchol ME, Wenthold RJ, Kelley MW (2006) Asymmetric localization of Vangl2 and Fz3 indicate novel mechanisms for planar cell polarity in mammals. J Neurosci 26:5265–5275.

Nicolson T (2005) The genetics of hearing and balance in zebrafish. Annu Rev Genet 39:9–22.

Nicolson T, Rüsch A, Friedrich RW, Granato M, Ruppersberg JP, Nüsslein-Volhard C (1998) Genetic analysis of vertebrate sensory hair cell mechanosensation: the zebrafish circler mutants. Neuron 20:271–283.

Popper AN, Fay RR (1993) Sound detection and processing by fish: critical review and major research questions. Brain Behav Evol 41:14–38.

Qian D, Jones C, Rzadzinska A, Mark S, Zhang X, Steel KP, Dai X, Chen P (2007) Wnt5a functions in planar cell polarity regulation in mice. Dev Biol 306:121–133.

Riley BB, Zhu C, Janetopoulos C, Aufderheide KJ (1997) A critical period of ear development controlled by distinct populations of ciliated cells in the zebrafish. Dev Biol 191:191–201.

Sakaguchi H, Tokita J, Müller U, Kachar B (2009) Tip links in hair cells: molecular composition and role in hearing loss. Curr Opin Otolaryngol Head Neck Surg 17:388–393.

Seiler C, Nicolson T (1999) Defective calmodulin-dependent rapid apical endocytosis in zebrafish sensory hair cell mutants. J Neurobiol 41:424–434.

Seiler C, Finger-Baier KC, Rinner O, Makhankov YV, Schwarz H, Neuhauss SC, Nicolson T (2005) Duplicated genes with split functions: independent roles of protocadherin15 orthologues in zebrafish hearing and vision. Development 132:615–623.

Shotwell SL, Jacobs R, Hudspeth AJ (1981) Directional sensitivity of individual vertebrate hair cells to controlled deflection of their hair bundles. Ann N Y Acad Sci 374:1–10.

Si F, Brodie H, Gillespie PG, Vazquez AE, Yamoah EN (2003) Developmental assembly of transduction apparatus in chick basilar papilla. J Neurosci 23:10815–10826.

Siemens J, Lillo C, Dumont RA, Reynolds A, Williams DS, Gillespie PG, Müller U (2004) Cadherin 23 is a component of the tip link in hair-cell stereocilia. Nature 428:950–955.

Söllner C, Rauch GJ, Siemens J, Geisler R, Schuster SC, Müller U, Nicolson T (2004) Mutations in cadherin 23 affect tip links in zebrafish sensory hair cells. Nature 428:955–959.

Tanimoto M, Ota Y, Horikawa K, Oda Y (2009) Auditory input to CNS is acquired coincidentally with development of inner ear after formation of functional afferent pathway in zebrafish. J Neurosci 29:2762–2767.

Tilney LG, Tilney MS, DeRosier DJ (1992) Actin filaments, stereocilia, and hair cells: how cells count and measure. Annu Rev Cell Biol 8:257–274.

Waguespack J, Salles FT, Kachar B, Ricci AJ (2007) Stepwise morphological and functional maturation of mechanotransduction in rat outer hair cells. J Neurosci 27:13890–13902.

Wang J, Mark S, Zhang X, Qian D, Yoo SJ, Radde-Gallwitz K, Zhang Y, Lin X, Collazo A, Wynshaw-Boris A, Chen P (2005) Regulation of polarized extension and planar cell polarity in the cochlea by the vertebrate PCP pathway. Nat Genet 37:980–985.

Wang Y, Guo N, Nathans J (2006) The role of Frizzled3 and Frizzled6 in neural tube closure and in the planar polarity of inner-ear sensory hair cells. J Neurosci 26:2147–2156.

Whitfield TT, Riley BB, Chiang MY, Phillips B (2002) Development of the zebrafish inner ear. Dev Dyn 223:427–458.

Wu YC, Ricci AJ, Fettiplace R (1999) Two components of transducer adaptation in auditory hair cells. J Neurophysiol 82:2171–2181.

Zine A, Romand R (1996) Development of the auditory receptors of the rat: a SEM study. Brain Res 721:49–58.